Electronic Supplementary Material (ESI) for Journal of Materials Chemistry A.

Supporting information for

# Carbonized carbon dots-modified starch aerogel for efficient solar-powered water evaporation

Xiaoshi Xu,[a] Qing Chang,[a]* Chaorui Xue,[a] Ning Li,[a] Huiqi Wang,[a] Jinlong Yang[a,b] and Shengliang Hu[a]*

[a] Research Group of New Energy Materials and Devices, North University of China, Taiyuan 030051, China
[b] State Key Laboratory of New Ceramics and Fine Processing, Tsinghua University, Beijing 100084, China

*Corresponding authors. changneu@gmail.com (Q. Chang), hsliang@yeah.net (S.L. Hu).

## Experimental section

### *Synthesis of carbonized carbon dots-modified starch aerogel (C-CDSA)*

Carbon dots (CDs) were prepared via our previously reported method.[1] A certain amount of the obtained CDs powder was dispersed in 24 mL of deionized water and continually stirred for 1 h. Then potato starch (3 g), ammonium persulfate (0.024 g) and N,N′-Methylene bisacrylamide (0.0288 g) were added. After being stirred for 30 min and treated with ultrasonic for another 30 min, the mixed solution was heated to 63 °C in a water bath and kept stirring to become uniform starch paste. The starch paste was poured into the mold and gelatinized at 90 °C for 15 min. The gelatinized sample was retrograded subsequently at 4 °C for 12 h and formed hydrogel. The obtained hydrogel was frozen at -20 °C in a refrigerator for 4 h and then thawed in water at room temperature for 1 h. After four freeze-thaw cycles and freeze-dried for 24 h, the carbon dots-modified starch aerogel (CDSA) was obtained. The obtained CDSA was put into a crucible and heated up to 270 °C for 1 h with a heating rate of 1 °C/min under argon atmosphere. The resulting carbonized CDSA was named as C-CDSA. For comparison, pure starch aerogel (SA) and carbonized starch aerogel (C-SA) were prepared using the same process with CDSA and C-CDSA except without adding CDs.

### *Characterization of the synthesized samples*

Scanning electron microscope (SEM) images were recorded using a FEI QUANTA FEG 400. The phase and crystallinity were analyzed using X-ray diffraction (XRD) on a Bruker D8 Advance diffractometer equipped with a Cu Kα X-ray source operating at 40 kV and 40 mA. X-ray photoelectron spectroscopy (XPS) spectra were recorded using a Thermo ESCALAB 250 equipped with a multichannel detector. Fourier-transform infrared (FTIR) spectra were measured on a Thermo Nicolet 360 FTIR spectrometer. The $N_2$-sorption isotherms were collected on a JW-BK300 apparatus. The specific surface area was measured using the Brunauer-Emmett-Teller (BET) method. The pore size distribution plots were obtained from the analysis of the adsorption branches of the isotherms using the Barrett-Joyner-Halanada (BJH) method. The density and porosity were measured via Archimedes principle. UV-vis-NIR absorption spectra were acquired by a Shimadzu UV3600 spectrophotometer with an integrated sphere. UV-vis absorption spectra were acquired by a Shimadzu UV-2550 UV-vis spectrophotometer. The water contact angle was measured on a Drop Shape Analysis System OCA20. The thermal conductivity of the sample was measured on XIATECH thermal conductivity coefficient instrument (TC3000E).

### *Water Evaporation measurements*

The solar-driven water evaporation was performed in a quartz container wrapped with thermal insulator polystyrene foam (28 °C in laboratory with relative humidity of 23%). The simulated sunlight irradiation was provided by a 300 W Xe arc lamp (CEL-PE300L-3A, CEAULIGHT, China). The light intensity was measured with the UV intensity meter. The mass change of water was recorded by an electrical balance. The temperature changes were measured using a dual-channel thermocouple. The infrared (IR) images were also captured via an IR camera (UTi80, UNT-T).

### *Evaporation test under acidic, alkaline, salty and organic pollutant condition*

The water solution with different pH values were adjusted by adding HCl or NaOH. Different concentrations of NaCl solution (3.5, 7, 10, 15, 20, and 25 wt%) were prepared. And methylene blue (MB, 15 mg/L) was used as organic pollutant solution. The procedure of the evaporation tests under these conditions were the same as that for pure water evaporation test.

### *Outdoor performance*

To evaluate the potential for practical application, outdoor water evaporation of the obtained C-CDSA in water and NaCl solution of 10 wt% under natural sunlight irradiation was carried out. This device was placed on the roof of the Engineering Center at North University of China on Mar. 10th 2022 (3~21 °C with relative humidity of 8~15%). The mass change of water was recorded from 9:00 to 17:00.

### *Calculation of solar-powered water evaporation conversion efficiency (η)*

The solar energy conversion efficiency was calculated according to the following equation:[2]

$$\eta = \dot{m}H_{LV}/C_{opt}q_0 \tag{S1}$$

where $\dot{m}$ is the evaporation rate of water under light illumination ($\dot{m} = m_{light} - m_{dark}$, $m_{dark}$ = 0.138 kg m$^{-2}$ h$^{-1}$ in our work), $H_{LV}$ is the equivalent vaporization enthalpy of water in evaporator, $C_{opt}$ is the optical concentration, $q_0$ is the power density of 1.0 sun (1 kW m$^{-2}$).

In this work, equivalent evaporation enthalpy $H_{LV}$ was first calculated according to the reported method in reference:[3, 4]

$$H_{LV} = \Delta H_{vap}m_0/m_g \tag{S2}$$

where $\Delta H_{vap}$ was the vaporization enthalpy of water at room temperature ($\Delta H_{vap,\ 28°C}$ = 2440 J K$^{-1}$ g$^{-1}$), $m_0$ was the evaporation rate of bulk water, $m_g$ was the evaporation rate of the samples. Notably, here the water and samples had the same surface area, and the evaporation experiments were tested under dark condition with the same environmental temperature and humidity.

Besides, the evaporation enthalpy of water in samples was also measured via differential scanning calorimetric (DSC).[3-5] The samples were placed in an open Al crucible and measured with heating rate of 5 °C/min under nitrogen flow flux (100 mL/min) in the temperature range from 0~200 °C.

***Calculation of heat loss***

*Heat loss by radiation*

The value of heat radiation was calculated according to Stefan-Boltzmann equation:[6]

$$J_{rad} = \varepsilon\sigma(T_{gel}^4 - T_{env}^4) \tag{S3}$$

where $\varepsilon$ is the emissivity (0.97),[7] $\sigma$ is Stefan-Boltzmann constant ($5.67 \times 10^{-8}$ W m$^{-2}$ K$^{-4}$). $T_{gel}$ is the steady-state temperature of the solar evaporator surface (41 °C for C-CDSA, 36 °C for C-SA), $T_{env}$ is the air temperature above the solar evaporator (39 °C for C-CDSA, 33 °C for C-SA) under 1.0 sun irradiation. The radiation heat was calculated to be 13.5 W m$^{-2}$ for C-CDSA and 19.2 W m$^{-2}$ for C-SA, which was about 1.35% and 1.92% of the input energy of 1.0 sun, respectively.

*Heat loss by conduction*

The value of heat conduction was calculated according to the following equation:[6]

$$J_{cond} = Q_{cond}/At = Cm\Delta T/At \tag{S4}$$

where $C$ is the specific heat capacity of water (4.2 kJ$^{-1}$ kg$^{-1}$ °C), $Q_{cond}$ is the heat energy conducted to bulk water, $t$ is the conductive time (1 h). The evaporator area ($A$) is $3.14 \times 10^{-4}$ m$^2$, and the water weight ($m$) is 4 g in this work. $\Delta T$ represents the increment of bulk water before and after irradiation for 1 h (which was obtained from Fig. 5a, 5 °C for C-CDSA, 7 °C for C-SA). The conduction heat was calculated to be 71.3 W m$^{-2}$ for C-CDSA and 104.0 W m$^{-2}$ for C-SA, which was about 7.13% and 10.4% of the input energy of 1.0 sun, respectively.

*Heat loss by convection*

The value of heat convection was calculated according to Newton' law of cooling:[6]

$$J_{conv} = h(T_{gel} - T_{env}) \tag{S5}$$

where $h$ is the convection heat transfer coefficient (5 W $m^{-2}$ $K^{-1}$).[8] The convection heat was calculated to be 10.0 W $m^{-2}$ for C-CDSA and 15.0 W $m^{-2}$ for C-SA, which was about 1.0% and 1.5% of the input energy of 1.0 sun, respectively.

The total heat loss was 9.5% for C-CDSA and 13.8% for C-SA.

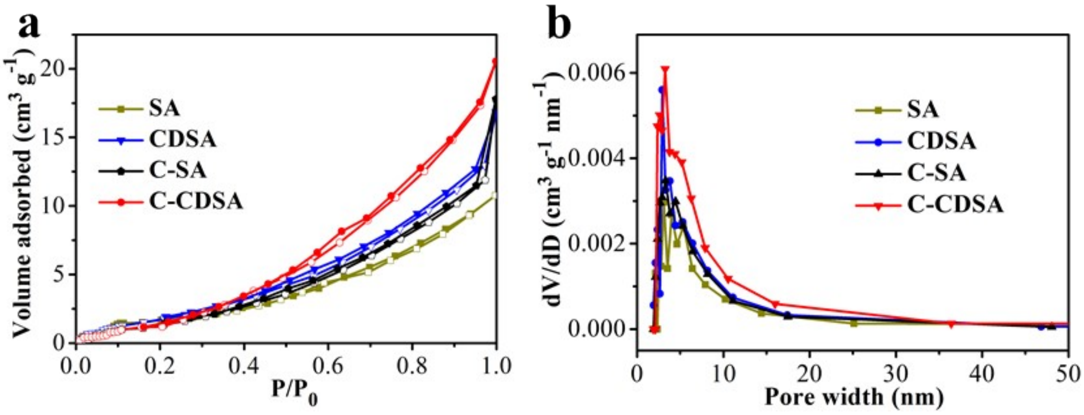

**Fig. S1.** (a) $N_2$ adsorption-desorption isotherms and (b) Pore size distribution curves of as synthesized samples.

**Table S1.** Physical parameters of as synthesized samples.

| Sample | $D_{BJH}$ (nm)$^a$ | $S_{BET}$ (m$^2$/g)$^b$ | $V_{spt}$ (cm$^3$/g)$^c$ |
|---|---|---|---|
| SA | 6.637 | 5.844 | 0.017 |
| CDSA | 7.335 | 5.979 | 0.026 |
| C-SA | 8.251 | 4.482 | 0.028 |
| C-CDSA | 14.14 | 4.125 | 0.078 |

[a] Pore size calculated by BJH method from adsorption branch of isotherms.

[b] Surface area calculated by BET method at relative pressure of $P/P_0$ =0.2

[c] Single point total pore volume calculated by the nitrogen amount adsorbed at $P/P_0$ = 0.999.

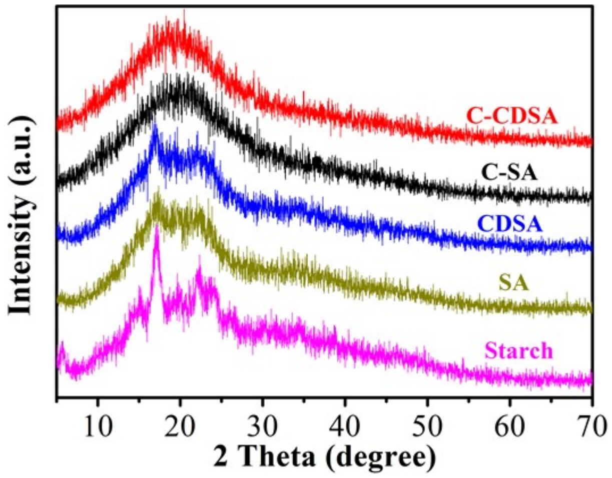

**Fig. S2.** XRD patterns of as synthesized samples.

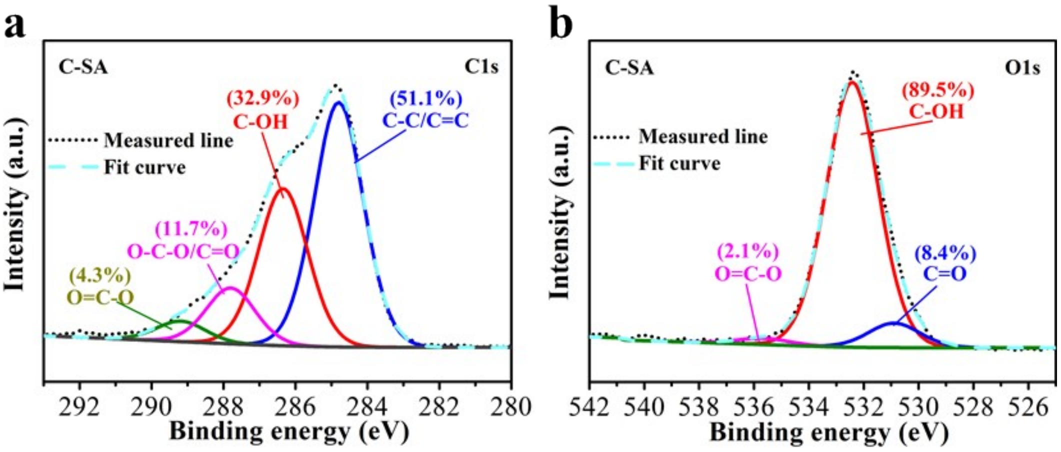

**Fig. S3.** High-resolution XPS spectra of C1s and O1s of C-SA.

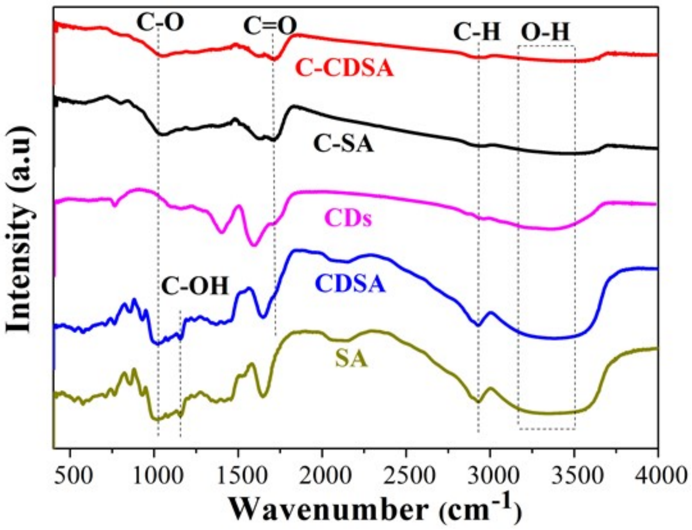

**Fig. S4.** FTIR spectra of as synthesized samples.

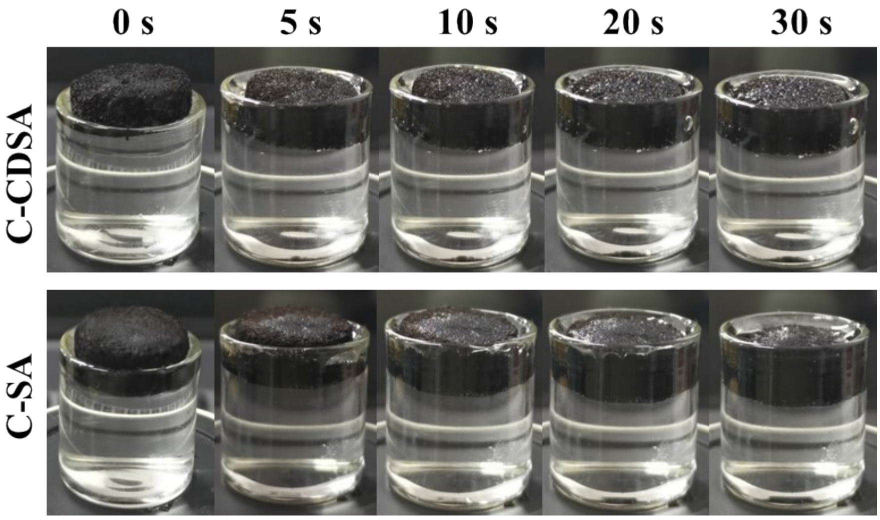

**Fig. S5.** Photographs of C-SA and C-CDSA floating on the water surface.

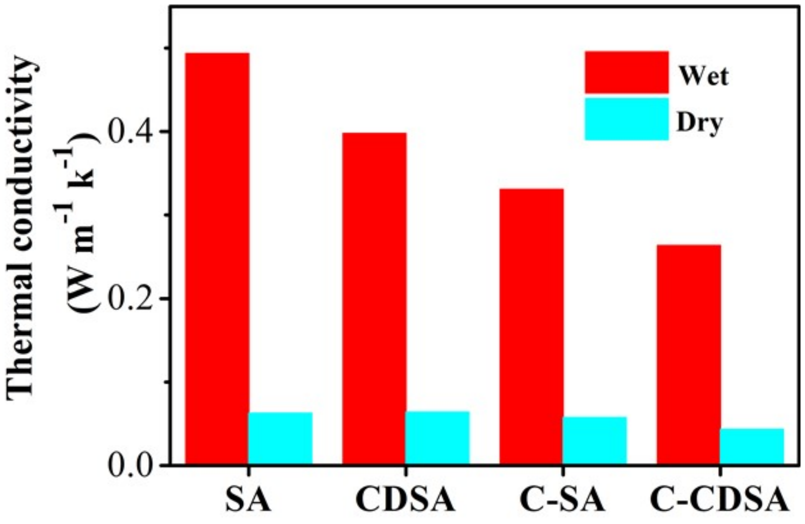

**Fig. S6.** Thermal conductivities of as synthesized samples under dry and wet conditions.

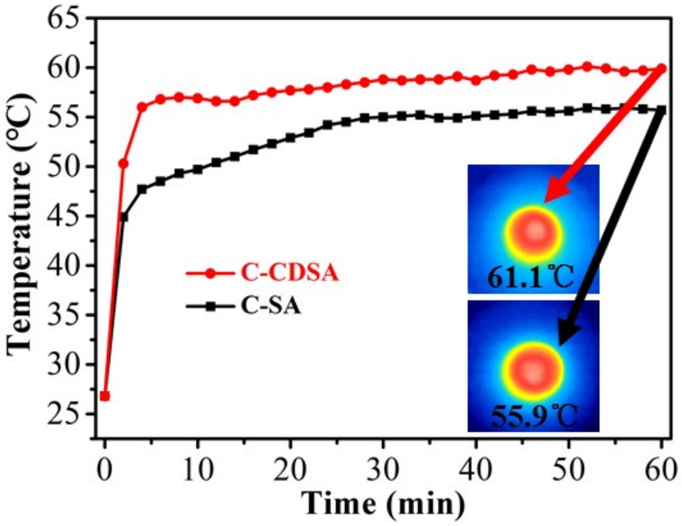

**Fig. S7.** Surface temperature changes of dry samples under 1.0 sun.

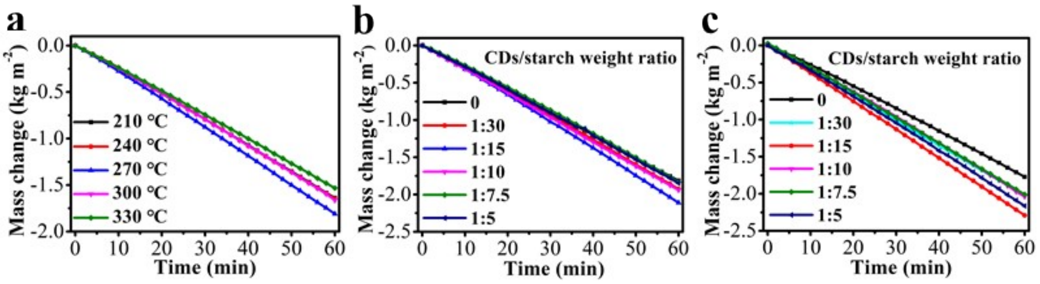

**Fig. S8.** (a) Water mass change over time of C-SA carbonized at different temperatures under air atmosphere. Water mass change over time of C-CDSA with different weight ratio of CDs to SA carbonized at 270 °C under (b) air and (c) argon atmosphere.

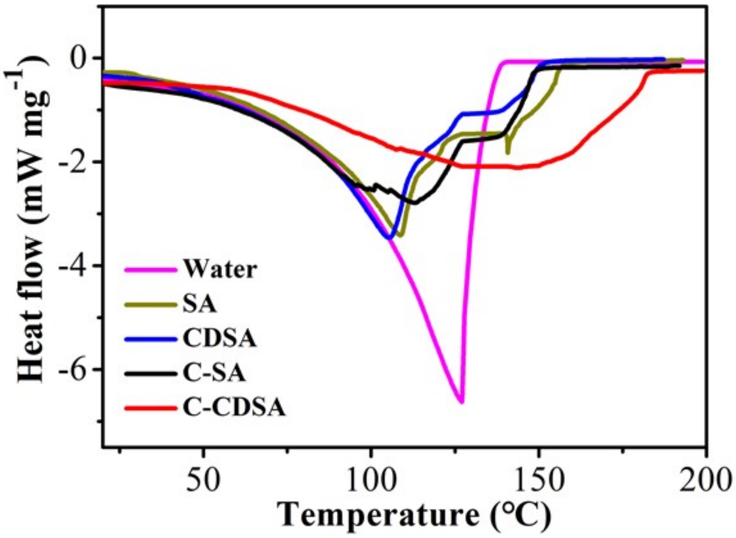

**Fig. S9.** DSC curves of the bulk water and water in the as synthesized samples.

**Table S2.** Summary of calculated equivalent evaporation enthalpy and DSC measurement results.

| | SA | CDSA | C-SA | C-CDSA | Water |
|---|---|---|---|---|---|
| Total mass (mg) | 79.9 | 84.6 | 53.4 | 71.1 | 62.7 |
| Water (mg) | 67.7 | 72.3 | 41.2 | 58.9 | 62.7 |
| Enthalpy via DSC (J/g) | 1856 | 1772 | 1736 | 1561 | 2487 |
| Calculated enthalpy (J/g) | 1809 | 1715 | 1698 | 1535 | 2440 |

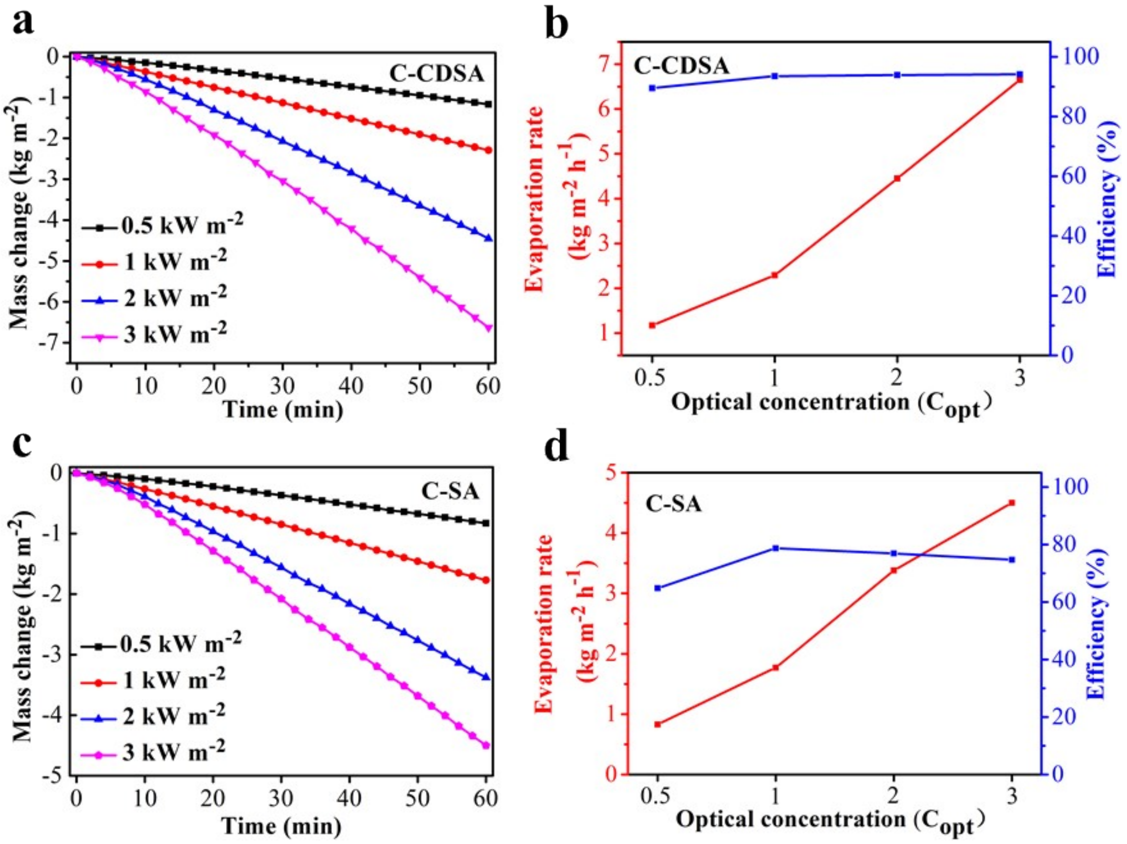

**Fig. S10.** The evaporation rates and corresponding energy efficiency of (a,b) C-CDSA and (c,d) C-SA under various irradiation intensity.

**Fig. S11.** Photograph of the moldy CDSA.

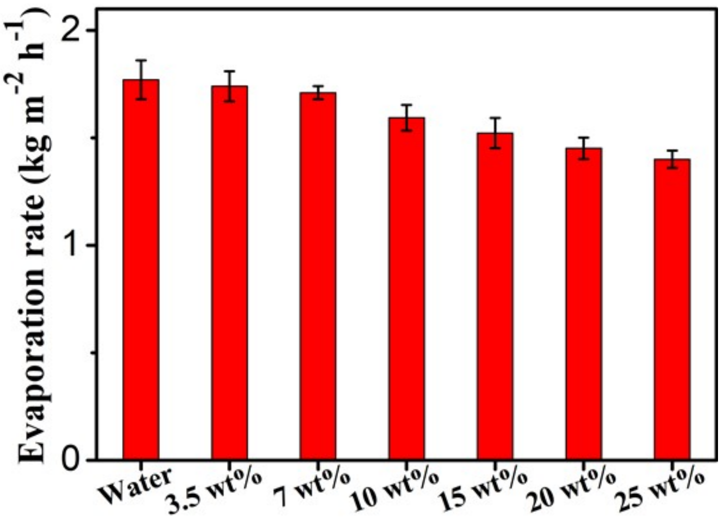

**Fig. S12.** Water evaporation rates of C-SA in different concentrations of NaCl solution.

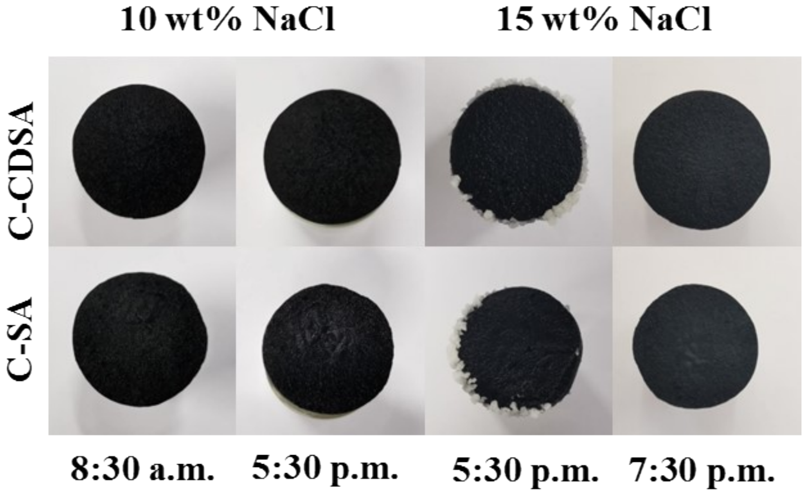

**Fig. S13.** Photographs of the samples in NaCl with concentration of 10 wt% and 15 wt% when exposed to outdoor from 8:30 to 19:30 under natural sunlight.

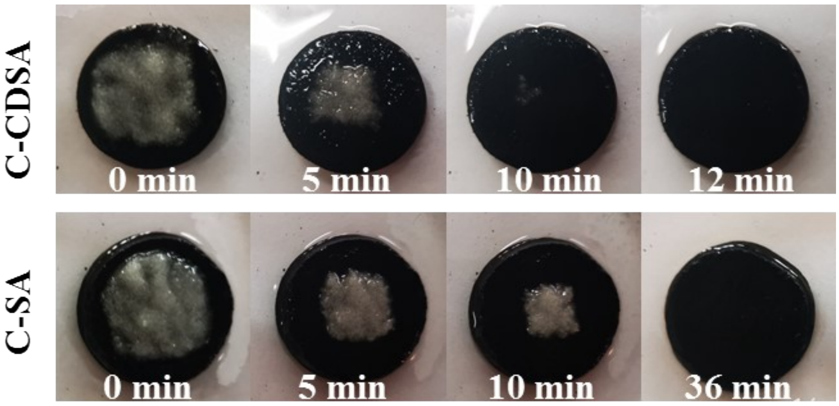

**Fig. S14.** Redissolving of solid NaCl on the surface of C-CDSA and C-SA.

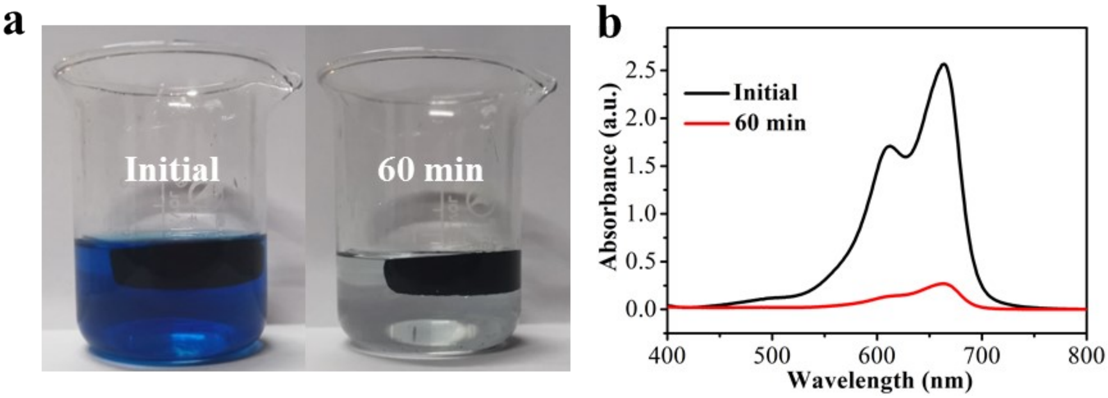

**Fig. S15.** (a) Photographs of bulk MB solution with C-CDSA before and after water evaporation test. (b) UV-vis absorbance spectra of bulk MB solution before and after water evaporation test.

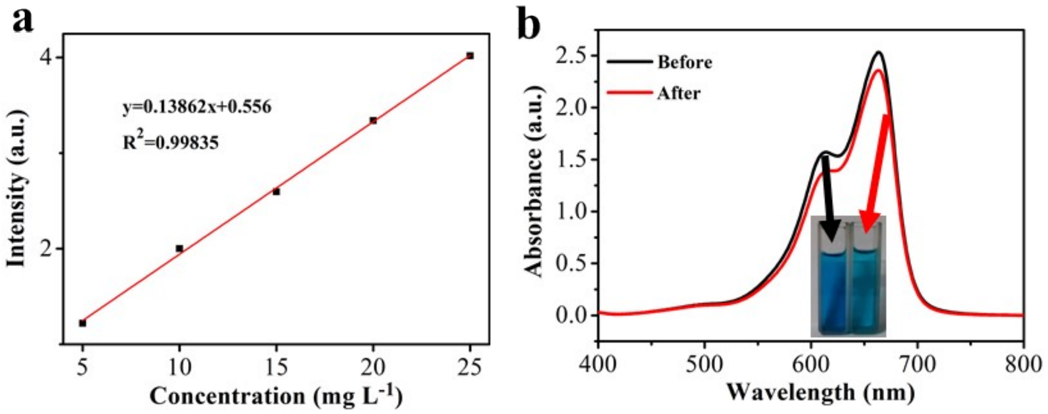

**Fig. S16.** (a) Calibration curve of concentrations of MB. (b) UV-vis absorbance spectra of original MB solution and ethanol solution used as the desorption agent for MB (Inset: the photographs of original and desorbed MB solution).

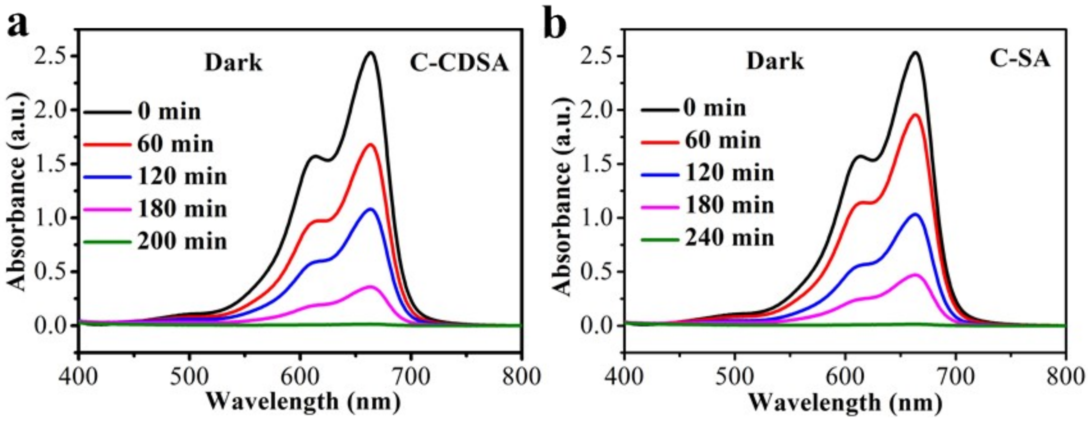

**Fig. S17.** The time-dependent UV-vis absorbance spectra of MB with (a) C-CDSA and (b) C-SA under dark.

## References

1. X. Meng, Q. Chang, C. Xue, J. Yang and S. Hu, *Chem. Commun.*, 2017, **53**, 3074-3077.
2. L. Zhang, B. Tang, J. Wu, R. Li and P. Wang, *Adv. Mater.*, 2015, **27**, 4889-4894.
3. F. Zhao, X. Zhou, Y. Shi, X. Qian, M. Alexander, X. Zhao, S. Mendez, R. Yang, L. Qu and G. Yu, *Nat. Nanotechnol.*, 2018, **13**, 489-495.
4. Y. Guo, X. Zhao, F. Zhao, Z. Jiao, X. Zhou and G. Yu, *Energy Environ. Sci.*, 2020, **13**, 2087-2095.
5. Q. Lu, W. Shi, H. Yang and X. Wang, *Adv. Mater.*, 2020, **32**, 2001544.
6. M.-Q. Yang, C. F. Tan, W. Lu, K. Zeng and G. W. Ho, *Adv. Funct. Mater.*, 2020, **30**, 2004460.
7. Y. Yang, R. Q. Zhao, T. F. Zhang, K. Zhao, P. S. Xiao, Y. F. Ma, P. M. Ajayan, G. Q. Shi and Y. S. Chen, *ACS Nano*, 2018, **12**, 829-835.
8. H. Ghasemi, G. Ni, A. M. Marconnet, J. Loomis, S. Yerci, N. Miljkovic and G. Chen, *Nat. Commun.*, 2014, **5**, 4449.